Drinking with the wind

Small scale SWRO-installation mechanically driven by wind energy

November 2008

Evgenia Rabinovitch

Faculty of Civil Engineering and Geosciences

Delft University of Technology

Drinking with the wind

Small scale SWRO-installation mechanically driven by wind energy

Master of Science Thesis in Civil Engineering and Geosciences

Evgenia Rabinovitch

November 2008

Committee:

Prof.ir. J.C. van Dijk	Delft University of Technology Sanitary Engineering Section
Dr.ir. S.G.J. Heijman	Delft University of Technology Sanitary Engineering Section
Dr.ir. J.Q.J.C. Verberk	Delft University of Technology Sanitary Engineering Section
Prof.dr. G.J.W. van Bussel	Delft University of Technology Wind Energy Section

Delft University of Technology

Sanitary Engineering
Department of Water Management
Faculty of Civil Engineering and Geosciences

"Yes we can." - Barack Hussein Obama II

Acknowledgements

This report is the final result of the Mater Thesis project of Sanitary Engineering Section at the Faculty of Civil Engineering and Geosciences at Delft University of Technology. The subject of this project is producing of drinking water with a small scale SWRO-installation mechanically driven by wind energy.

I would like to thank all people involved in this project, especially the members of my graduation committee. Prof. Hans van Dijk gave me the opportunity and the freedom to execute this project for my graduation. Bas Heijman was my supervisor and was always available for theoretical discussions as well as practical advise. I would like to thank Jasper Verberk for his support and encouragements. Prof. Gerard van Bussel shared his knowledge about wind energy that was very useful for my thesis.
I would like to thank Peter de Moel, Tony Schuit and Patrick Andeweg for their support and involvement in the project during the testing period in Delft and beyond.

"Drinking with the wind" was financially supported by Mr. and Mrs. Grootscholten, who collected the first money to start the project. But I am also very thankful for the inspiration and motivation Mr. Grootscholten gave to me to execute this project.
Aqua For All and DEMO also gave a substantial financial contribution to this project.
I would like to thank Hatenboer-water for their financial contribution and especially for all the practical knowledge and facilities I was allowed to use during the building of the RO-instalaltion. A special thank you goes out to Carel Averink and all the people at the workshop that always had time and will to help me.

The realization of the first prototype on Curacao was supported by Waterplatform Nederlandse Anitllen & Aruba (WNAA). Special thanks to people at Aqualectra for their assistance during building up and testing of the first prototype in Curacao. I would like to thank especially Ben Statia and Manuel Pereira for their contribution to the project on Curacao.

Much gratitude goes out to Keith Meyerscough, my roommate, for his great help and moral support.

Last but not least I would like to show my great gratitude to Nick Olthof and Friso Bos. Thank you for sharing the good times and the bad times. Without you this project would never have been such a great success.

Evgenia Rabinovitch,
Delft, November 2008

Drinking with the wind

Small scale SWRO-installation mechanically driven by wind energy

E. N. Rabinovitch[1], S.G.J. Heijman[1,2], F.W.C.. Bos[1], N. Olthof[1], J.Q.J.C. Verberk[1], G.J.W. van Bussel[1], J.C. van Dijk[1],
[1] Delft University of Technology, Stevinweg 1, 2628CN Delft, The Netherlands, S.G.J.Heijman@tudelft.nl
[2] Kiwa Water Research, Groningerhaven 7, 3430BB Nieuwegein

Abstract

Sea water is often the only available water source in arid, remote areas. Reverse osmosis (RO) desalination is the most energy efficient technology to treat saline water for drinking water purposes. Nevertheless it is still an energy intensive process, traditionally powered by fossil energy sources. Due to increasing costs and environmental drawbacks of fossil energy sources it becomes economically feasible to use renewable energy sources. In this project wind energy is used to power an RO-installation. Direct, mechanical drive is used instead of an electric drive to prevent energy losses by conversion and expensive electrical energy storage.
The first prototype of a small scale RO-installation mechanically driven by wind power was designed, built and tested. The operation was variable due to the characteristics of the wind power supply. The process controls were operating mechanically/hydraulically without the use of electricity. To prevent delaminating of the RO-membranes a fresh flush was included. The fresh flush was activated hydraulically when the wind speed dropped below a certain level and the recovery was controlled mechanically as well.

Keywords

Reverse osmosis, desalination, renewable energy, small scale water treatment, wind energy

Introduction

In arid areas, with scarce fresh water resources, but sufficient saline or brackish water, desalination is the only method to produce drinking water.
Desalination can be done using thermal methods or membrane separation technology. In table 1 the specific energy consumption for different desalination methods is given. The most energy efficient technology to desalinate sea water is reverse osmosis (RO) [1].

Table 1 Specific energy consumption of various desalination methods [1-3]

Desalination technology	**kWh/m³**
Multi Stage Flash (MSF)	18
Multiple Effect Distillation (MED)	15
Vapour Compression (VC)	11
Reverse Osmosis (RO) (large scale)	3
Freezing	16

Traditionally fossil energy is used to power RO-desalination. However, fossil energy sources are becoming increasingly scarce and the costs are increasing [4]. Additionally, CO_2 emissions are involved in using fossil energy sources. A combination between desalination and renewable energy sources (RES) is therefore the next step in desalination technology. Renewable energy sources like hydropower, wind and solar energy have already been in use for centuries. Kalogirou [5] gives an extensive overview of possible desalination methods driven by RES and emphasizes the growing demand for such applications worldwide. An overview of existing small scale RES

(wind, solar) desalination in the Mediterranean region is given by Tzen et al. [6]. It is found that PV-RO (32%) is the most used combination in the region, followed by wind-RO (electrical drive). Especially for remote areas, without reliable water supply and limited access to fossil energy sources, a combination between desalination and RES is becoming progressively feasible for drinking water production [4, 7-9].

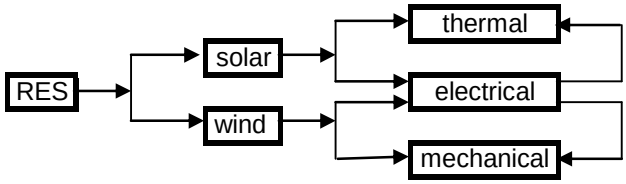

Figure 1 Renewable energy sources (RES)

From wind and solar energy sources different types of power can be obtained (figure 1).
Solar energy can be used directly as thermal energy to distillate saline water. But it is also possible to transform solar energy into electric energy by photovoltaic's (PV) and use the electricity to drive an electric pump [10].
Wind energy can also be used directly to drive a high pressure pump of a RO-installation mechanically. The kinetic energy of the wind is then transformed into mechanical energy of the high pressure pump.
RES is transformed into electrical energy and expensive and unreliable electrical energy storage (batteries) is needed [11, 12]. Furthermore, energy losses occur with each energy conversion [4].
The main disadvantage of PV's is the high investment costs, especially of the batteries. Solar energy is available for maximal 8 hours a day. Therefore electrical energy storage is needed to overcome periods with insufficient solar radiation. Wind energy is variably available during most of the day, provided that the right location is chosen with sufficient wind regime. The (electrical) energy storage, for wind driven RO-installations, is therefore much smaller compared to the storage for solar powered RO-installations.
In this article the wind energy source in combination with RO is going to be discussed in more detail, while other renewable energy sources, such as solar, geothermal energy, hydropower and biomass energy are not evaluated.
Miranda and Infield [13] investigated a RO-system powered by wind energy without batteries, minimizing investment and operating costs. A theoretical model was developed to predict the performance of the system with variable operation without use of batteries, but no prototype was built. At the same time emphasis was laid on the unknown consequences on the membranes due to variable operation of RO membranes [7, 13].
The idea to use kinetic energy of the wind to drive the high pressure pump of the RO system is also described by Witte et al. [14]. Motivated primarily by prevention of the energy losses that occur with kinetic energy conversion into electricity, storage of it and then converting it back to shaft power to drive the pump. Also Feron [7] investigated the direct drive and the operational complications, due to variable power availability, in detail. Three operational configurations were analyzed: RO-plant operating at constant conditions, RO-plant operating under varying conditions and RO-plant operating with varying membrane area. One of the recommendations to make the wind powered RO-desalination more feasible, is to investigate the larger pressure variation on the membranes to reach a larger water production due to larger power input. In both cases [7, 14] no prototype was built. Witte et al. [14] had built a prototype of a vapor compression desalination installation based on a compression pump directly connected to a windmill.
Liu et al. [15] described a prototype for brackish water desalination, where a multi bladed wind mill drove a piston pump directly. The pressure depended on the available wind power. The recovery and flux were kept constant by regulating the feed pressure. Solar cells were used to obtain electricity for the pressure measurements and the process controls.

The objective of this research project was to design, build and test a small scale RO-installation mechanically driven by wind power. This installation was designed for stand alone operation for remote areas without electricity available. The control and operation of the installation were designed fully mechanically or hydraulically.
The installation has been tested in Curacao, the Netherlands Antilles.

Methods and Materials

Prototype

In this research project wind energy was used to power a small scale SWRO-installation. Direct mechanical transmission was used between the wind turbine and the high pressure pump. The mechanical transmission made the generation and storage of electricity unnecessary. The control and operation of the installation were done mechanically and hydraulically, to exclude any use of electricity in the system. As the wind power was variable, the operation mode was also variable, in contrast to conventional RO-installations. The variable loading was possible due to a low hydraulic load on the membranes. The recovery was kept low and constant, at a maximum of 20% in order to prevent scaling. Also an energy recovery was used to reuse energy from the concentrate in the same way it is commonly done in larger RO-installations.
The nominal production of the RO-instalaltion was designed at 5 m^3 a day at an average wind speed of 7 m/s. This production is enough for a small village of 500 people in a developing country. The installation was designed to produce a maximum of 10 m^3/day at an average wind speed of 12 m/s.

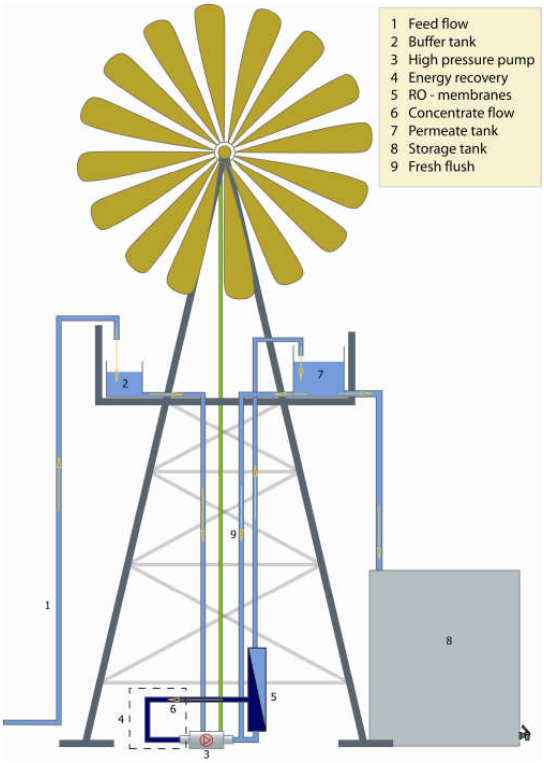

Figure 2 Schematics of the first prototype


Figure 3 First prototype on Curacao, Dutch Antilles

In figure 2 a schematic drawing of the prototype is depicted.
The pretreated feed flow (1) of 2 m³/h was supplied to a buffer tank (2), with a volume of 30 liters. The buffer tank was situated at 10 meter height and served as a security against running dry of the high pressure pump. When the buffer tank was empty it mechanically activated a brake to stop the operation of the installation (figure 4).

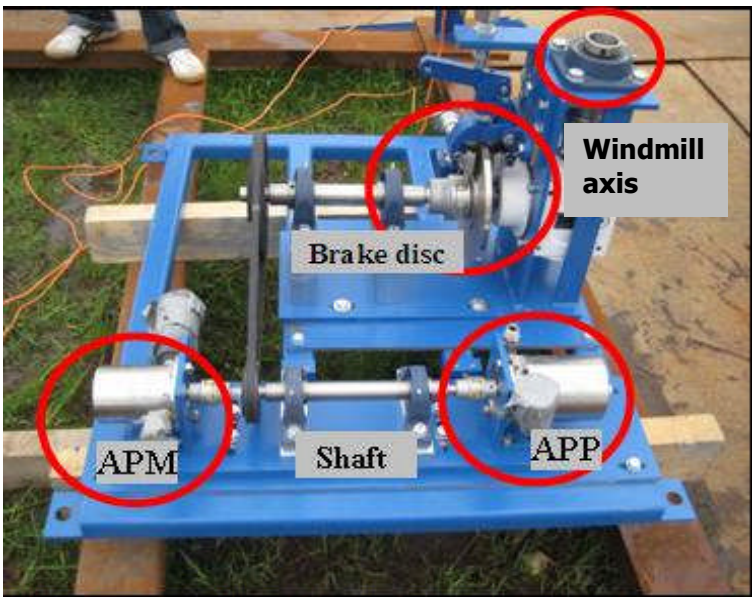

Figure 4 Mechanical transmission

The high pressure pump (3) was a piston pump (APP) and was directly connected to the windmill axis with a mechanical transmission. Also an energy recovery system (4) was used (APM), connected to the same axis as the high pressure pump (figure 4). The high pressure pump and energy recovery system were connected by shaft and were also used to control the recovery.
After the pressure was built up and the osmotic pressure of the feed water had been overcome, permeation started. The permeate was first stored in the permeate tank (7) with a volume of 100 liters, situated at 10 meters height. When the permeate tank was filled it overflows and the permeate is stored in a larger fresh water storage tank (8). The volume of the tank of 25 m³ was determined by the volume of water to overcome wind still periods or maintenance periods when the windmill was out of operation, for a maximum of 5 days.
When the wind speed was too low to drive the pumps or there was a possibility of the pump to run dry, the system was stopped and a fresh flush was activated (9). This happened automatically after opening a needle valve manually. The permeate from the permeate tank flushed the feed side of the membranes, to prevent delaminating of the membranes due to natural osmosis.
The small scale RO-installation was designed using only off-the-shelve components. The membranes used were 4 SWC1-4040 (4 inch) Hydranautics membranes. The membranes were placed in serial order and there was a possibility to use either 2 or all 4 elements during the testing period. The flow and pressure measurements were done hydraulically (Alaxa, type: HK and ENFM, type: kl. 1.18 respectively). The conductivity measurements were done by a portable EC-meter on batteries.
To achieve the high pressure needed for RO-desalination a Danfoss APP1.5 high pressure pump is used and APM 1.2 is an energy recovery turbine constructed on the same axis (figure 4).
The recovery was kept low and constant by using the Danfoss APP/APM piston pumps so that the chance for scaling is minimized and no concentrate valve is necessary.

The APM has also a function of an energy recovery system. This kind of turbine is used in large and medium installations, to minimize the energy requirement for RO-desalination [16].

The feed water had to be pretreated to prevent damage to the pumps and membranes. Conventional pre-treatment, like a beach well, is recommended in order to prevent fouling. The feed had to be delivered at 1 bar pressure to be able to fill the buffer tank that served as a running dry security for the high pressure pump. The product water is corrosive due to low hardness, causing damage to storage and distribution facilities. Therefore the product water needs a post treatment using a limestone filter, to increase the hardness of the permeate. Pre-treatment, post treatment and brine discharge are not discussed further in this paper, as they are no subject to the design of the small wind driven SWRO-installation. Bio-fouling or other long term fouling was not investigated in this research as well.

Wind energy

The average wind speed can be used to estimate the theoretical kinetic power of the air mass flowing through an area swept by the rotor blades:

$$P_{kin} = \frac{1}{2} * \rho_{air} * A * v^3 \quad (1)$$

P_{kin} =kinetic power [W]

ρ_{air} = air density (1.2 kg/ m³, pressure 1 atm and temperature 20° C)
A = surface rotor blades [m²]
v = wind speed [m/s]

From equation 1 it is clear that power is dependant on the third power of wind velocity [4, 7]. Due to energy losses caused by the transition of kinetic energy to mechanical energy, the maximum theoretical power according to Betz' law is [17]:

$$P_{max} = C_p * P_{kin} \quad (2)$$

P_{max} = mechanical power [W]

C_p = aerodynamic efficiency [-]

Where the theoretical maximum of value of C_p is $\frac{16}{27} * 100\% \approx 59.3\%$ [18]. In practice the C_p for the multi-bladed windmills is between 0.3 and 0.4 [18]. For this prototype a value of 0.35 is assumed.
Further losses occur due to the mechanical bearings and mechanical coupling and are estimated for this prototype at a total of 12% (table 2).

Table 2 Energy losses of the mechanical coupling [19]

Component	Energy loss [%]	Amount	Total [%]
gear box	3	2	6
V-belt	1	1	1
bearing	0,5	10	5
Total			**12**

Taking this into account the available mechanical power for the pump is:

$$P_{mech} = \eta_{mech} * C_p * P_{kin} \quad (3)$$

P_{mech} = mechanical power [W]

η_{mech} = mechanical efficiency $(1 - \frac{12}{100} = 0.88)$

With a wind speed of 6 m/s, the rotor surface $A = \pi * \left(\frac{1}{2} * 5\right)^2$ combined with equations 1, 2 and 3, the theoretical mechanical power delivered by the windmill is 784 W.

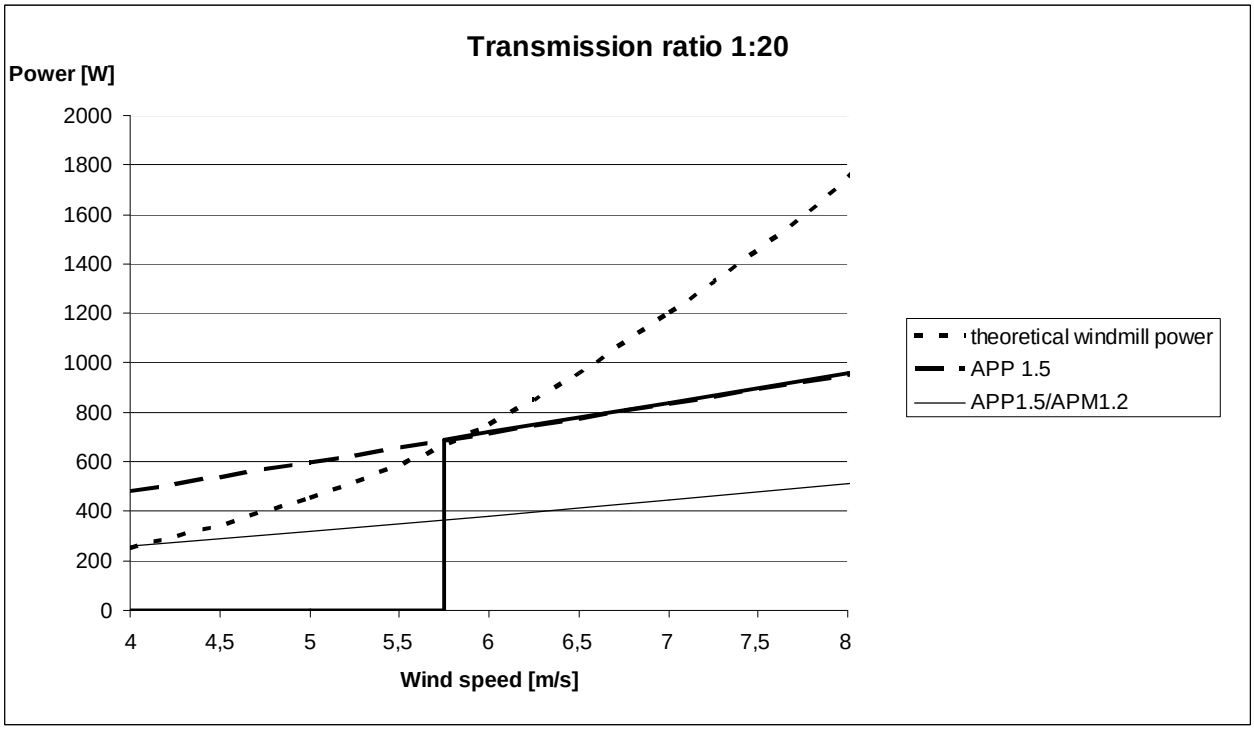

Figure 5 Power requirements APP/APM and available power windmill

This corresponds to the theoretical net power delivered by the windmill at the same wind speed from figure 5. The relatively small difference between the calculated value and one presented by the manufacturer is due to a different pump connected to the windmill originally.

To identify the wind regime a lengthy period of wind speed measurements is needed for a certain location. Not only the range of the wind speed available on that location is measured, but also the duration of a certain wind speed is important to know as well. The wind regime can be described using the Weibull function [18]. The Weibull distribution is characterized by the shape parameter (k) and the scale parameter (c). The cumulative probability distribution function (equation 4) is indicating the time fraction or probability that the wind speed is smaller than or equal to a certain wind speed (v'). The frequency of the wind speed is represented by the probability density function (equation 5).

$$F(v) = P(v \leq v') = 1 - \exp\left[-\left(\frac{v}{c}\right)^{k}\right] \quad (4)$$

$$f(v) = \frac{F(v)}{dv} = \frac{k}{c} * \left(\frac{v}{c}\right)^{k-1} * \exp\left[-\left(\frac{v}{c}\right)^{k}\right] \quad (5)$$

$$c = \frac{\bar{v}}{\Gamma(1 + \frac{1}{k})} \quad (6)$$

$F(v)$ = cumulative distribution function [-]

$f(v)$ = probability density function [s/m]

c = scale parameter [m/s]

k = shape parameter [-]

$\bar{v}$ = average wind speed [m/s]

$\Gamma(1 + \frac{1}{k})$ = gamma function (for k=3.5, $\Gamma(1 + \frac{1}{k}) = 0.899747$ [18])

When the long term measurements of the wind speed on location are not available at the right height the $1/7^{th}$ power law is used [20] to calculate the wind speed at the height of the rotor:

$$v = v_r (z_x/z_r)^{\alpha} \quad (7)$$

v = unknown wind speed at a given height [m/s]

v_r = known wind speed at a reference height [m/s]

z_x = given height [m]

z_r = reference height [m]

α = stability coefficient, approximately $1/7^{th}$ ($\approx 0{,}143$)

A representative Weibull distribution of the wind speed for the island of Curacao is depicted in figure 6, with k= 3.5 and an average wind speed of 6 m/s, found in literature and derived using equation 7 [18, 20]. The scale parameter (c) is calculated using equation 6. From the F (v) curve it is clear that on Curacao the wind speed is higher than or equal to 6 m/s for 50 % of the time. From the f (v) it is also evident that wind speed of 6 m/s is the most frequent speed at the location.

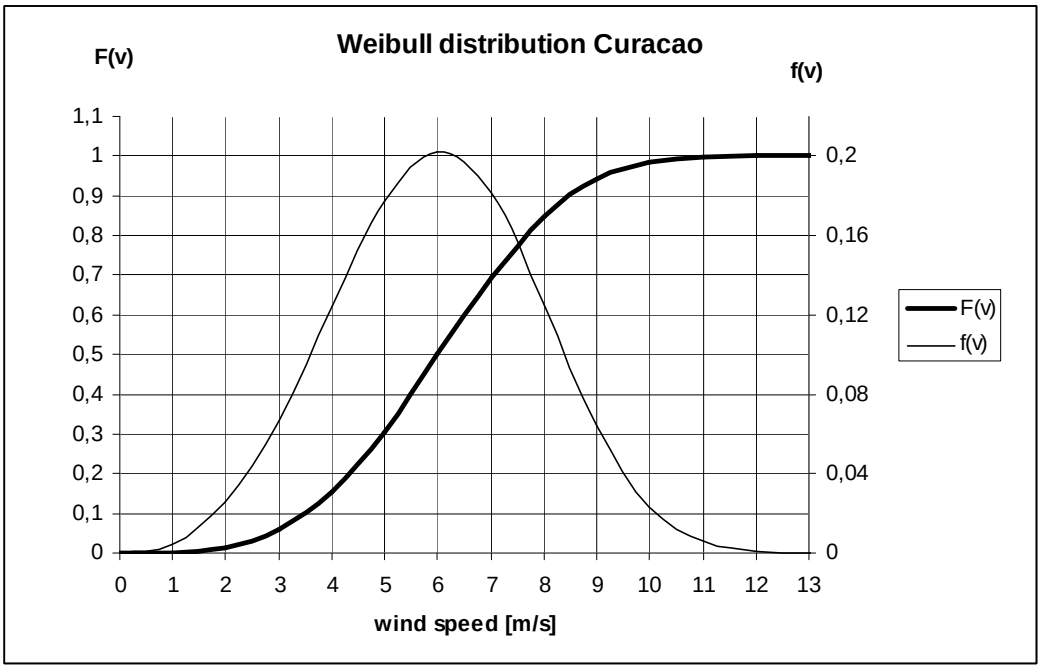

Figure 6 Wind speed distribution on Curacao

Wind turbine

A horizontal axis, high solubility wind turbine (figure 3), manufactured by MOLINS DE VENT TARRAGÓ (type: M 5015), was used to power the RO installation. The height of the tower was 15 m and the diameter of the rotor was 5 m. According to the specifications of the manufacturer, theoretical available power provided by the windmill at different wind speed is shown in figure 5. Originally the windmill was driving a groundwater pump with a translating axis. This axis was altered in a rotating axis to drive the high pressure pump. From the rotor axis a gear box transmission at right angle was connected with a vertical axis. At the ground level the vertical axis was connected with a horizontal axis in the same way. This horizontal axis is connected with a V-belt drive to the axis of the APP/APM combination.
The total transmission ration of the windmill axis to the pump was initially 1: 20 [21]. On the horizontal axis a brake disc is constructed that was put on manually or when the buffer tank runs dry (figure 4).
The mechanical power extracted by the rotor from the wind is equal to mechanical power exerted by the pump [18]. In this design with a feed flow of 0.625 m³/s and a design pressure of 60 bar the design wind speed of 6.5 m/s was calculated using equation 8.

$$P_{mech\_rotor} = P_{mech\_pump}$$

$$\eta_{mech} * C_p * \frac{1}{2} * \rho_{air} * A * v^3 = Q * \rho_{water} * g * H \quad (8)$$

Q = flow [m³/s]

ρ_{water} = density of water (1000 kg/m³)

g = acceleration of gravity (9.8 m/s²)

H = lifting head [m]

To determine the starting point of the operation the maximum required torque for the high pressure pump (APP) is calculated using equation 9. From the technical specifications of the pump manufacture, the torque is determined to be 10.6 Nm, at the rotation speed of 2890 rpm ($\Omega = \frac{2 * \pi * 2890}{60} = 302.6$ rad/s), power of 3210 W and operating pressure of 60 bar.

$$T = \frac{P}{\Omega} \quad (9)$$

T = torque [Nm]
P = power [W]
Ω = rotation speed [rad/s]

The torque is assumed to be constant at each rotation speed at the same operating pressure of 60 bar. Using this assumption and assuming that the rotational speed increases linearly with the wind speed as in the original configuration, the power demand of the high pressure pump is calculated as function of the wind speed at different rotation speed of the pump (figure 5). It can be seen that the power provided by the windmill is larger than the power consumed by the high pressure pump of the RO system. This means that the actual rotational speed of the new windmill-pump combination will be larger than in the original configuration, and will be such that a balance between power provided and power consumed is established again.
The same calculation was done for the combination APP/APM, when energy recovery system is delivering power from the concentrate the torque is equal to 5.9 Nm. The rotation speed of the pump and subsequently the power demand is dependant on transmission ratio between the rotor of the windmill and the pump.
In figure 5 the theoretical available power, generated by the windmill connected to the original pump, is shown as a function of wind speed. Also the power demand of the high pressure pump (APP) and the APP with energy recovery system (APM) are shown at the transmission ration of 1:20. Before the working point at approximately 6 m/s (V_{in}) the windmill stood still and no power extraction occured from the wind by the rotor. At the moment that windmill delivered sufficient torque the pump started to build up pressure. After the pump is started the power output of the windmill is equal to power demand of the pump plus the energy losses. The rest of the kinetic energy available in the wind is not transferred into mechanical energy, making the energy conversion less efficient. In the beginning of the operation there was no pressure yet and the energy recovery system (APM) did not provide energy back from the concentrate flow. After the pressure was built up and the osmotic pressure of the feed water was overcome, production of the permeate started. After building up the pressure, the APM recovered power from the concentrate as well and therefore the torque needed to keep the pump in operation is lower. The wind speed at which the production of water stopped is equal to 4 m/s (V_{stop}) as can be seen in figure 5 from the intersection of the APP/APM curve with the power curve of the windmill.

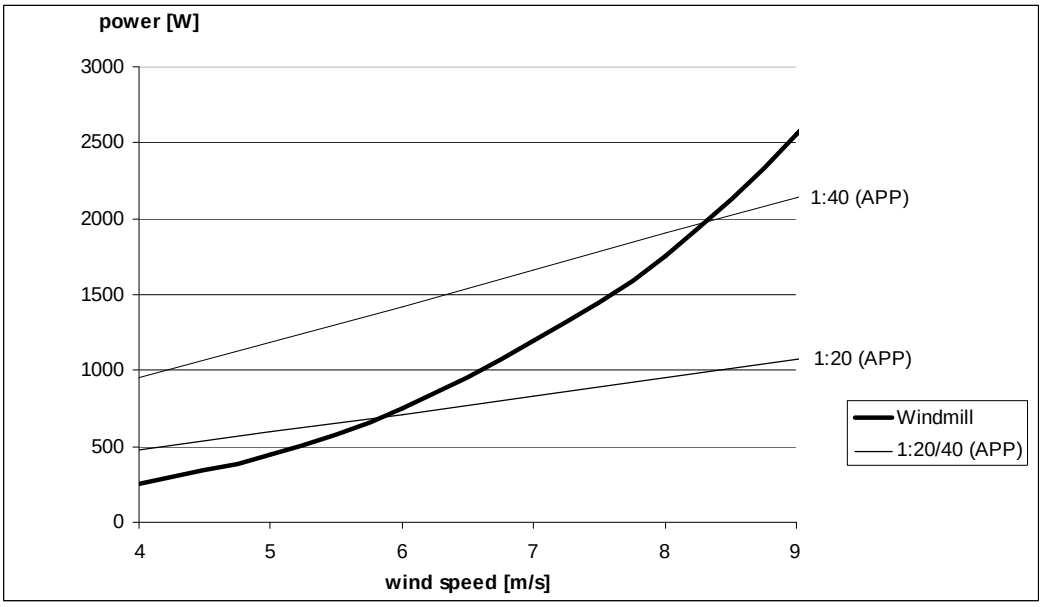

Figure 7 Power curves at different transmission ratios

In figure 7 the power curves of the pump at transmission ratio of 1: 20 and 1: 40 are shown. The initial transmission ratio was chosen to be 1: 20, to limit the maximal rotation speed of the pump. Later on this transmission ratio was changed to 1:40, to limit the minimal rotation speed of the pump. The torque needed for the pump is higher with higher transmission ratio; accordingly the working point is at a higher wind speed as well. From figure 6 it is clear that a higher wind speed occurs less often (≥ 8 m/s for 15% of the time) and leads to decrease in running time of the pump.

Recovery

Due to volume difference between the APP and APM pumps (figure 8) a nearly constant recovery is maintained. The low recovery of approximate 20 % keeps the concentration of the concentrate below the saturation concentration of soluble salts [22] in order to prevent scaling. Therefore no chemicals (acids) or anti-scalants were needed during the operation. Also the osmotic pressure of the feed flow is almost constant in the system with this low recovery. The salt concentration in the feed water will rise up with a maximal 25% in the last element of the installation (range of osmotic pressure π = 30 to 38 bar, calculated using DuPont Manual [23]).

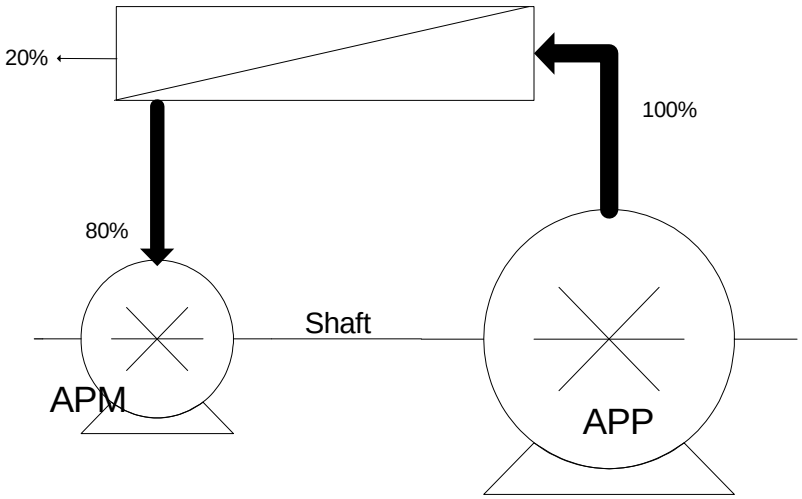

Figure 8 APP/APM combination with fixed recovery

Concentration polarization

Concentration polarization (CP) is a phenomenon of an increased salt concentration at the feed side of the membrane. Increase in salt concentration occurs because of the salt rejection of the membrane and a stagnant layer near the membrane wall that prohibits the mixing of it with the bulk of the feed flow. Three factors are important in occurrence of this phenomenon:

- The recovery determines the actual concentration in the bulk solution in the feed spacers in the membrane elements. Keeping recovery low (< 20%) means that the salt concentration will stay below the saturation concentration and the risk of scaling is minimised (C_m).
- A higher flux means a higher concentration polarisation (J).
- The cross velocity has to be high enough to cause more turbulent flow and keep the thickness (δ) of the stagnant boundary layer as thin as possible (k).

Concentration polarization (β) can be calculated using equation 10:

$$\beta = \frac{C_m - C_p}{C_f - C_p} = \exp\left(\frac{J}{k}\right) \qquad (10)$$

β = concentration polarization [-]

C_m = salt concentration at membrane surface [g/ m³]

C_p = salt concentration of permeate [g/ m³]

C_f = salt concentration of feed [g/ m³]

J = water flux [m³/ m² s]

k = mass transport coefficient [m/s]

The concentration of the product water is relatively low and can be neglected in equation 10. A high concentration polarization can lead to scaling and decrease of the flux and higher energy consumption. In the design the combination of APP/APM controls the concentration polarization. The recovery is fixed by the difference in volume of the pumps (figure 8). The flux and the cross flow velocity are proportionally dependant on rotation speed of the high pressure of the pump.

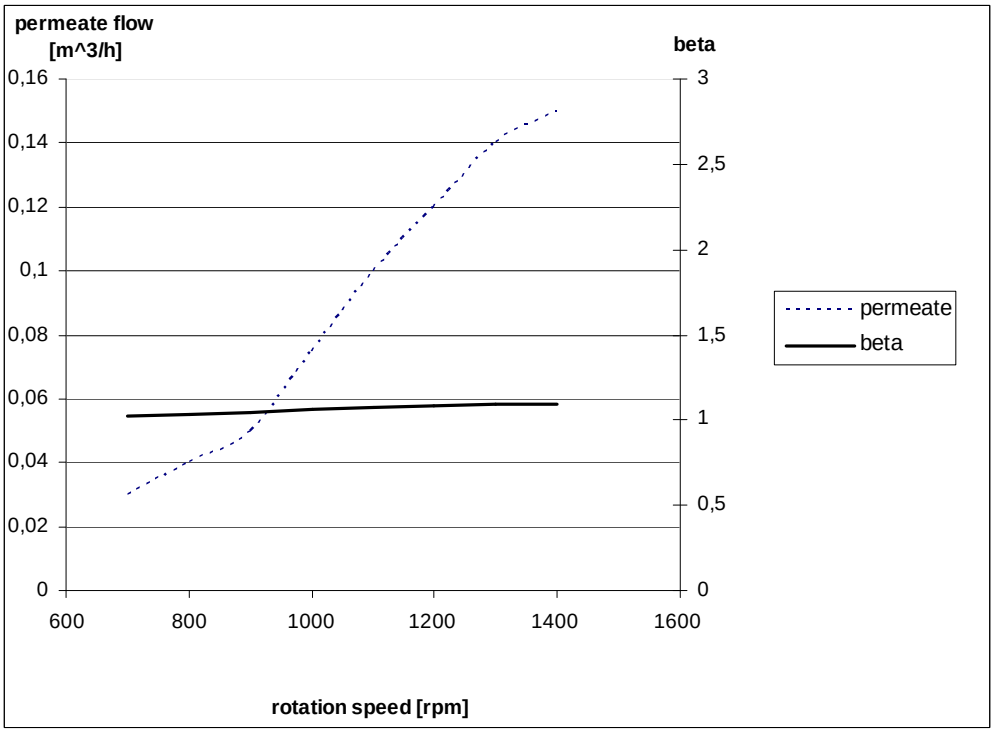

Figuur 9 Concentration polarization at variable flow calculated by IMSdesign

In figure 9 the concentration polarization as function of rotation speed of the pump is shown. With increasing cross flow velocity the turbulence of the flow increased as well, making the laminar layer thinner. The concentration polarization (β) stays below 1.2.

Experiments

Laboratory set up

The recovery was tested in laboratory of Sanitary Engineering (DUT), with artificial salty water using electric motor (EM) to drive the APP/APM pumps. The salt water had 35000 ppm of TDS, made by dissolving NaCl in tap water.

$$\gamma = \frac{Q_p}{Q_f} * 100\% \qquad (11)$$

γ = recovery

Q_p = permeate flow [m³/h]

Q_f = feed flow [m³/h]

The recovery was calculated, using equation 11, for the rotation speed between 700 and 1400 rpm of the pump. The feed flow and the product flow were measured with flow meter 1 and flow meter 2, respectively.

The effectiveness of the fresh flush was tested in the laboratory using the same experimental set up as for the recovery tests. The permeate tank was put at 11 meters height. After the operation was stopped, the concentrate valve was opened manually to flush the feed side of the membrane with permeate. The conductivity of the concentrate flow was measured with a portable EC-meter (ExStik II). The conductivity (EC) to TDS ratio was: TDS= 0.6 EC.

The flushing ratio of the membrane elements was calculated with equation 12.

$$F = \frac{V_{permeate} - V_{dead}}{V_{element}} \quad (12)$$

F =flushing ratio [-]

$V_{permeate}$ =permeate volume [L]

V_{dead} =dead volume of the pipes (7 L)

$V_{element}$ =volume of the elements (4 L per element)

Experimental set-up Curacao

The water production and quality were tested on location at RO-plant Fuik (Curacao, Dutch Antilles) in an area where the wind velocity is not disturbed by trees or high buildings. The exact wind data for the location was not available beforehand but an average wind speed was assumed to be 7 to 8 m/s, at the height of the rotor.

The wind driven RO-installation made use of pre treated sea water of the existing RO-plant. The pressure of feed water was around 2 bar, which was more then sufficient to fill the feed tank. The concentrate discharge of the wind driven RO-installation was also connected to the existing brine discharge at the RO-plant Fuik. The chemical analysis of the feed water can be found in table 3.

Table 3 Chemical composition of a sample of feed and concentrate water from WindRO Fuik.

Chemical parameters	Feed	Concentrate
Temperature [°C]	30,5	31,8
Conductivity [µS/cm]	46900	59240
pH [-]	7,6	7,5
Turbidity [NTU]	0,7	0,8
Chloride [mg/l]	23309	31481
Calcium [mg/l]	460	603
Carbonate [mg/l]	0	0
Bicarbonate [mg/l]	143	195
Sulfate [mg/l]	3775	4800
Sodium [mg/l]	13270	16330
Kalium [mg/l]	440	650

During the experiments the product water was discharged into a storage tank. The level of the water was registered every 15 minutes.

The conductivity of the product water was measured by taking samples every 5 minutes from the permeate tap.

The wind speed was measured using HOBO speed smart sensor and logged by the HOBO micro station data logger. The wind meter was situated at the height of 12 meters at the windmill tower.

To compare the actual concentration polarization (CP) to the projected one of figure 9, the clean water permeability of the membranes, the permeate flux, temperature and pressure (TMP) were measured on location in Curacao. Equation 13 was used to verify the projected value of the CP.

$$NDP = \frac{J * \mu}{K_w} = TMP - \pi_{mem}$$

$$\beta = \frac{C_{mem}}{C_{bulk}} \approx \frac{\pi_{mem}}{\pi_{bulk}} \quad (13)$$

NDP = net driving pressure [Pa]
J = permeate flux [m³/m²s]
μ = absolute viscosity [Pa s]
K_w = membrane water permeability ($2.46*10^{-15}$ m)
TMP = Trans Membrane Pressure [Pa]
C_{mem} = concentration at the membrane surface [mg/l]
C_{bulk} = concentration of the bulk [mg/l]
π_{mem} = osmotic pressure at membrane surface [Pa]
π_{bulk} = osmotic pressure of the bulk [Pa]

The saturation index (SI) is used to calculate if the scaling of bivalent salts occurs. When SI>0 the concentration of salts is above saturation concentration and precipitation can occur. When SI<0 there is no danger of exceeding the saturation concentration. The SI is calculated using equation 14 [24]:

$$SI = \log \frac{IP}{K_{sp}} \quad (14)$$

SI = saturation index [-]
IP = ion product [mol/l]
K_{sp} = solubility product [mol/l]

To determine specific energy consumption the feed pressure was measured and calculated using equation 15 [25].

$$E = \frac{P_f}{3600 * 1000 * \eta * \gamma}$$

$$E_{rec} = \frac{P_f}{3600 * 1000 * \gamma} * \eta_{rec} * (1 - \gamma)$$

$$E_{specific} = E - E_{rec} \quad (15)$$

E = energy consumption [kWh/m³]
P_f = feed pressure [Pa]
γ = recovery (20%)
η = efficiency pump (88%)
E_{rec} = energy recovery [kWh/m³]
η_{rec} =efficiency energy recovery (33%)
$E_{specific}$ = specific energy consumption [kWh/m³]

Results and discussion

Recovery

The development of the recovery with increasing rotation speed of the pump is given in figure 10. The experiments were executed twice in the laboratory under identical circumstances to reproduce the data. From figure 10 it is clear that recovery increased with an increase of the rpm of the pumps and is between 10% and 20% over the range of minimum and maximum rpm's for the pumps. However as the rpm's increased, the increase of the recovery flattened out at a maximum of 20 %. The results showed that even at larger rotation speeds, the recovery was fixed and stayed low. There is relatively larger increase of recovery in the lower range of rotation speed. This can be attributed to leakage of the pumps, that have a larger influence on the permeate production, relatively small at lower rpm's. Thus this leakage is influencing the recovery rate relatively more than at higher rotation speeds. The absolute leakage was calculated using equation 16 and was found to be 45 l/h.

$$Q_{loss} = \frac{\Omega_1}{\Omega_2} * Q_2 - Q_1 \qquad (16)$$

Q_{loss} = leakage flow [l/h]

Q_1 = feed flow at Ω_1 (30 l/h)

Q_2 = feed flow at Ω_2 (150 l/h)

Ω_1 = minimal rotation speed of the pump (700 rpm)

Ω_2 = maximum rotation speed of the pump (1400 rpm)

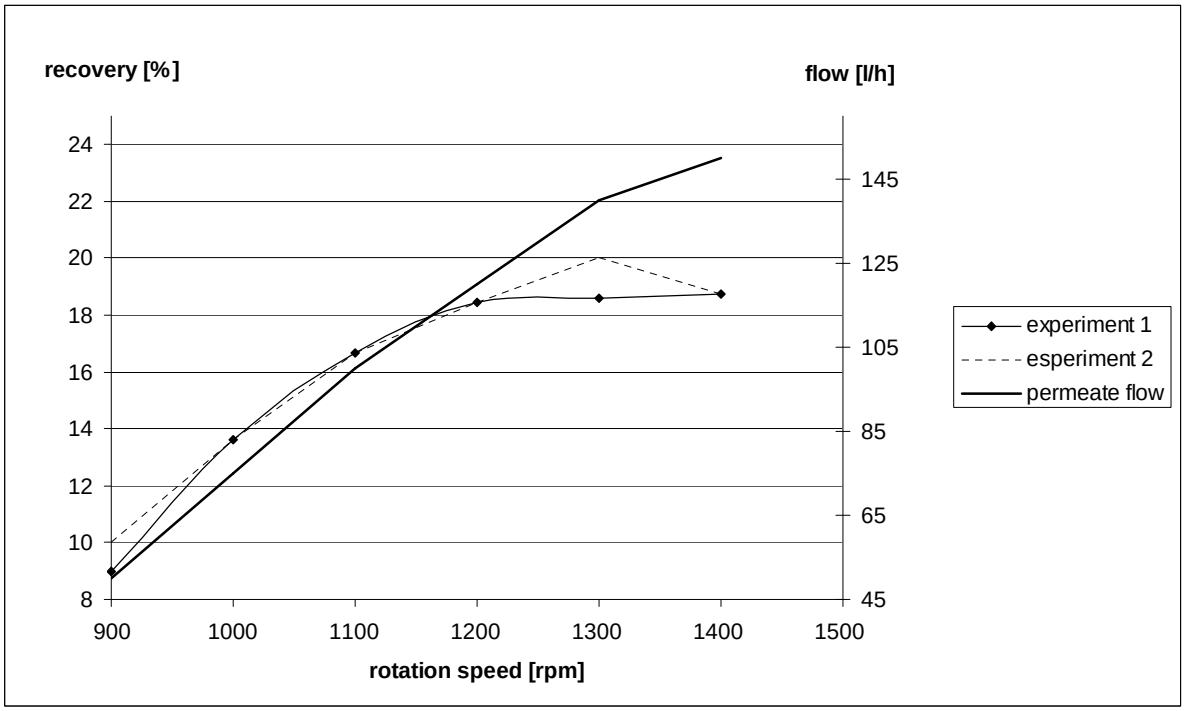

Figure 10 Recovery as function of rotation speed of the pump

Fresh flush
The fresh flush was tested in laboratory after 10 minutes of operation of the pumps at 1400 rpm and the result can be found in figure 11. It is clear that after the pumps are shut down, the operating pressure dropped rapidly to 0 bar. When the pressure was below 1 bar, the fresh flush started due to the hydrostatic pressure of 1 bar from the permeate tank. The conductivity, measured in the concentrate flow, dropped gradually from almost 70 mS/cm to close to the conductivity of the permeate (2.6 mS/cm). This indicates that after the driving pressure drops below 1 bar, the water from the permeate tank flushed the feed side of the membrane, preventing natural osmosis damaging the membranes. The elements are flushed with 100 L permeate in 40 minutes time. The flushing ratio was calculated using equation 12 (for 4 elements) and the membranes were flushed approximately 6 times.

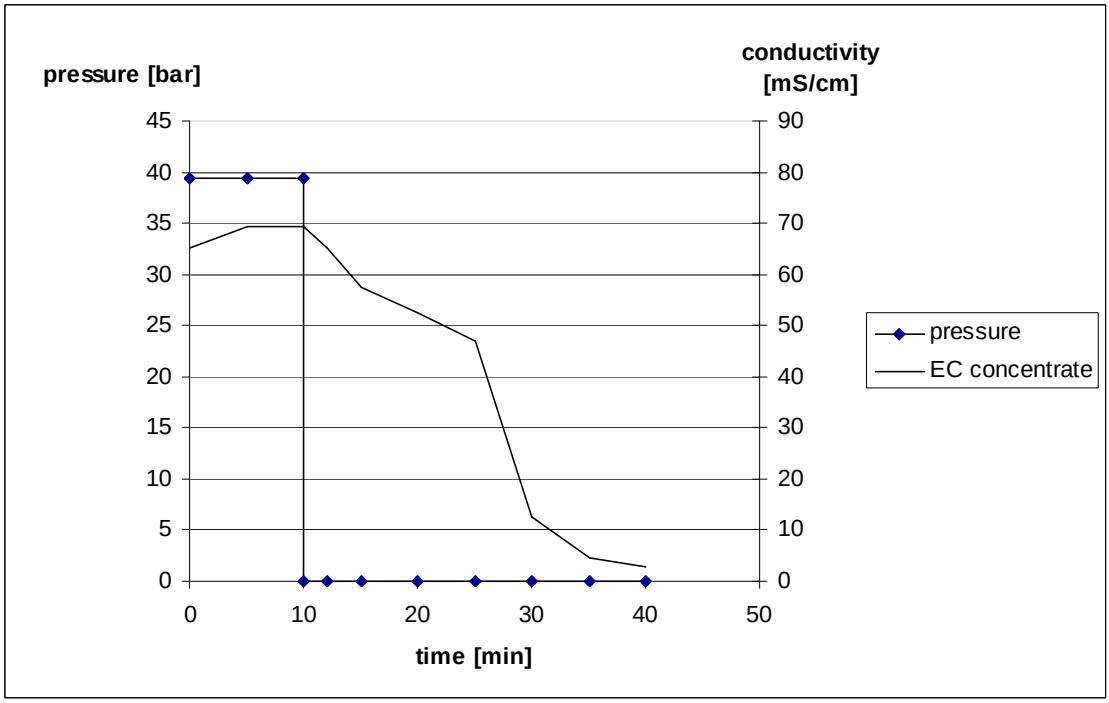

Figure 11 Effectiveness fresh flush

Water production
During the testing on location the wind speed, feed pressure and the permeate flow were measured continuously and are shown in figure 12. A more or less direct relation between wind speed (available power), pressure delivered by the high pressure pump and the permeate flow is observed. The differences can be explained by measuring inaccuracies and a delay in the system due to many transmissions in the system. The osmotic pressure of the feed water was 30 bar. The difference between the osmotic pressure and feed pressure is the net driving pressure (NDP). The permeate production is proportionally dependant on NDP. When NDP is 0 bar, there is no production. But even when the NDP is very small there is still some production that is equal to 1.5 m^3/day as can be seen in figure 12.

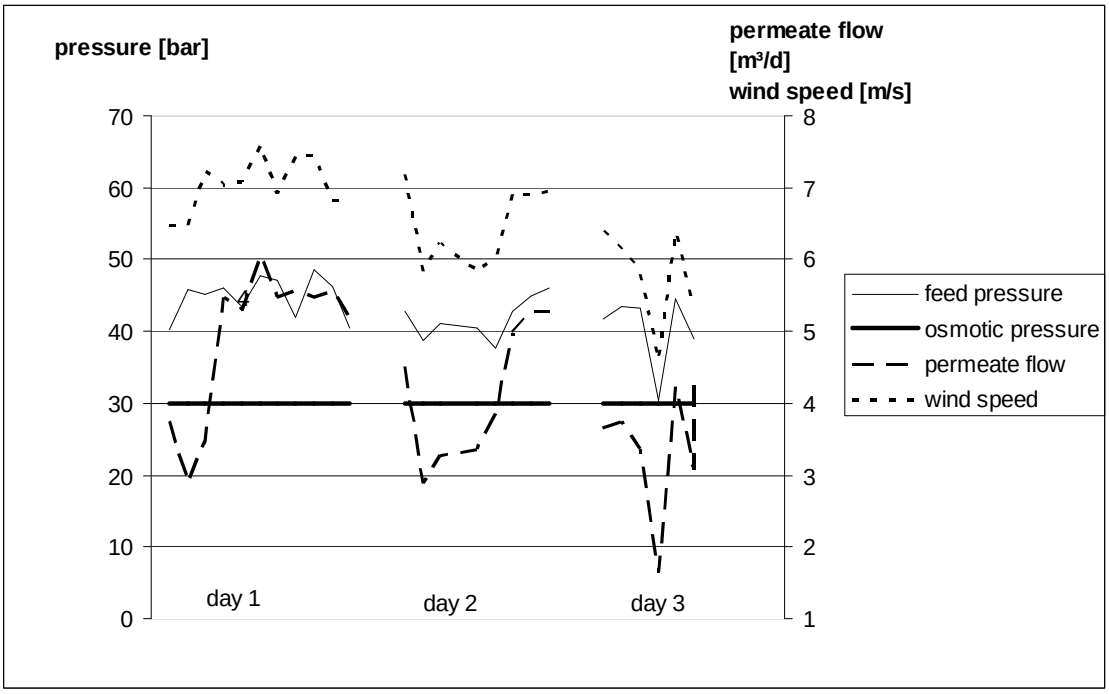

Figure 12 Relation between wind speed, permeate flow and pressure

In figure 13 the relation between wind speed and production is shown in more detail. The production increased with larger wind speed. From the theory (equation 1) the production was expected to be proportional to the third power of the wind speed. From the results the production is proportional to less then third power of wind speed. This can be explained by the less efficient power extraction by the windmill due to the interaction with the pump (equation 8). Therefore the relation between the available wind speed and the water production, as shown in figure 13, is a hybrid form between the third power and linear function. The curve is almost linear by the narrow range of the wind speed available on location and therefore optical flattening out of the results. The average production measured on location was approximately 0,2 m³/h resulting in a daily production of approximately 5 m³/day at average wind speed of 7 m/s. This shows that is possible to produce the designed amount of product water with variable operation. The maximum production of 10 m³/day was not reached due to insufficient wind power available at this location.

The concentration polarization (CP) was calculated with equation 13 to be β=1.03 at a flux of 0.23 m³/h , $\mu = 7.57*10^{-4}$ Ns/m² , π =30 bar, TMP= 46.25 bar. This shows that concentration polarization was low and the chance for scaling was minimal. The Saturation Index (SI) of bivalent salts was calculated for $CaCO_3$ using the concentrations measured in the concentrate flow, K_{sp} =4.96*10 $^{-9}$, IP=6.65*10 $^{-10}$ and substituted in equation 14. The result was SI= -0.87 <0. For $CaSO_4$ the saturation index was calculated the same way and was equal to -0.97 (with K_{sp} =7.1*10^{-5} and IP=7.63*10^{-6}) This shows that even at a high flux the concentrations stayed below saturation concentrations, minimizing the risk of scaling. The average specific energy consumption was 5.2 kW/ m³ and was calculated using equation 15 with an average P_f =42.8 bar. This is relatively low specific energy consumption for a small scale installation and slightly higher then the specific energy consumption in conventional large scale RO-installations (see table 1).

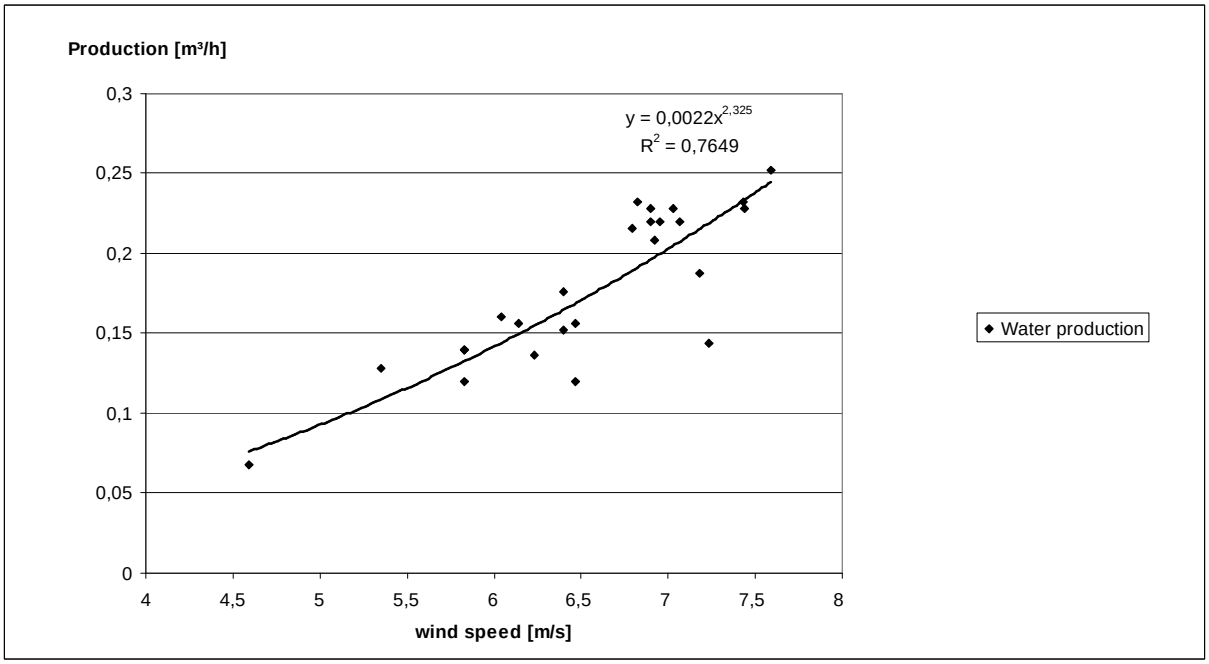

Figure 13 Water production as function of the wind speed

Water quality

During the experiments on location at Curacao the quality of permeate was measured by taking samples every 5 minutes. The relation between the wind speed and TDS, calculated from EC measurements, in the product water is given in figure 14. It shows a decreasing salt concentration with increasing wind speed. This is a result of an increased flux due to larger operating pressure, in accordance with the theory of salt passage.

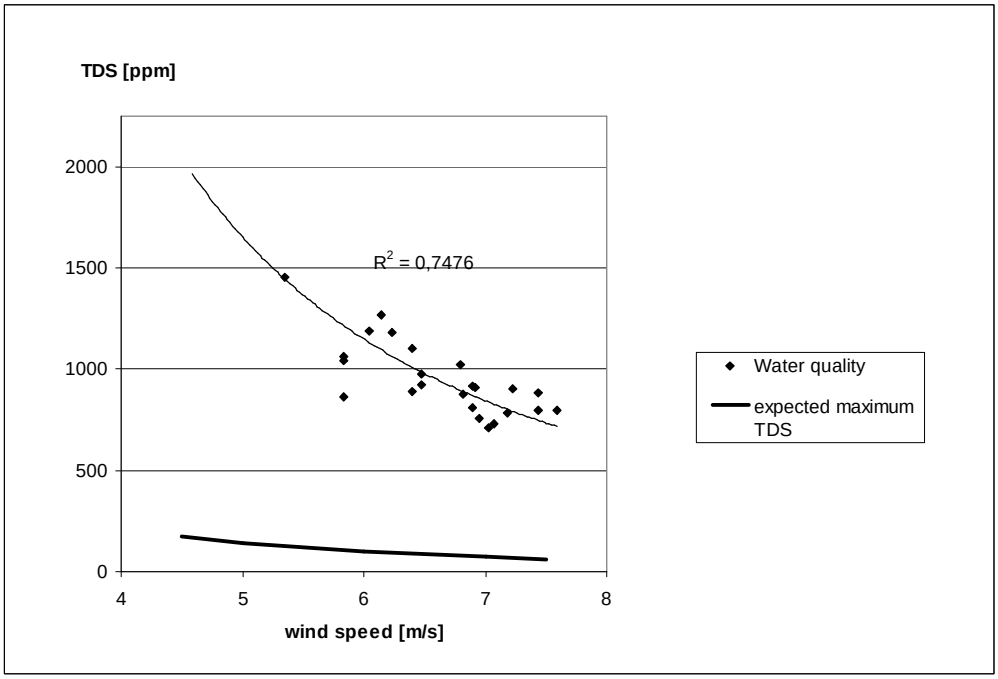

Figure 14 Salt concentration in permeate as function of the wind speed.

The product water quality was insufficient for drinking water purposes (>500 ppm), but high enough to use this water for irrigation purposes (< 1,200 ppm).
The concentration in the product water was calculated from the permeate of both membrane elements together and was found to be higher then expected. The expected TDS should have been below 500 ppm and the measured value was between 600 and 1500 ppm, depending on the flux. Figure 15 shows the salt passage of the membranes at various wind speed. The salt passage lies between 2% and 3% at a higher wind speed because the diffused ions are more diluted by a higher flux. This is 4 to 6 times higher then the maximum salt passage (0.5%) mentioned by the manufacturer of the membranes (Hydraunatics). Also both permeate flows from the elements were measured separately and it was discovered that one of the membranes was leaking. The difference between the elements in salt concentration was a factor 5 at a high flux, with 0.5% salt passage accounted for the uncompromised membrane and 5.5 % salt passage for the leaking one. This confirms the observation that one of the membranes performed insufficient. In case all of the elements had a salt passage according to manufacturer specifications (<0.5%) the product water quality would have been TDS ≤ 175 ppm.

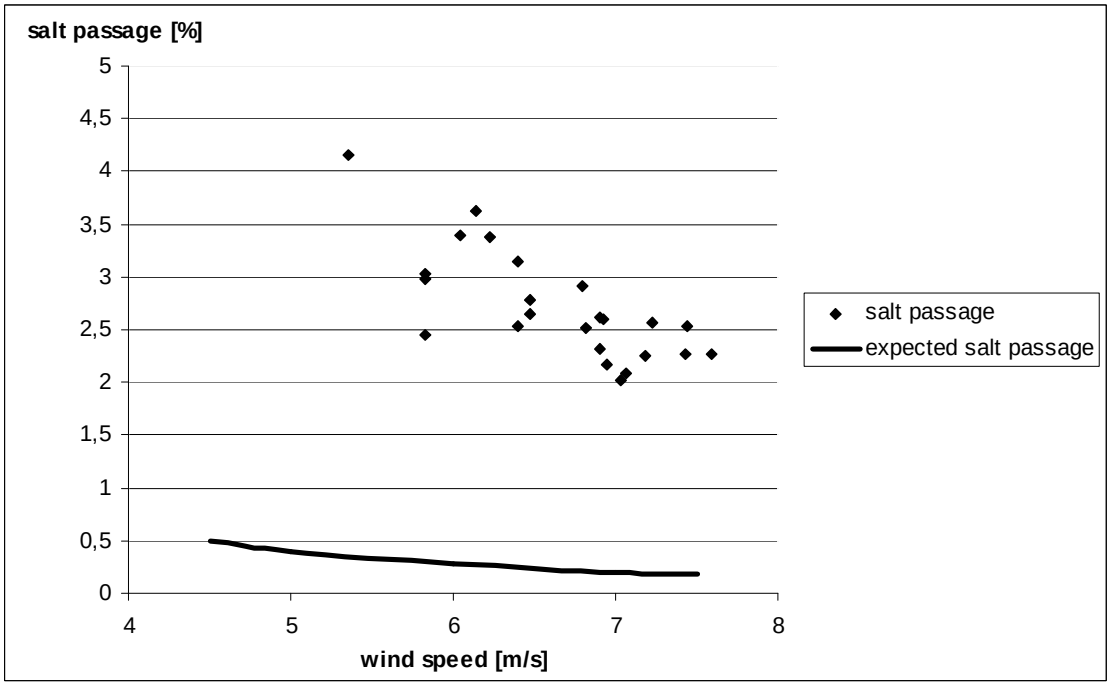

Figure 15 Salt passage of the membranes

Conclusions and recommendations

The first prototype of a small scale RO-installation mechanically driven by wind power was successfully designed, built and tested. The operation varied due to the characteristics of the wind power supply. The operation controls were done exclusively mechanically/hydraulically without any use of electricity. The fresh flush was activated hydraulically and the recovery was controlled mechanically as well.
The production of nearly 5 m³ a day was reached at a measured average wind speed of 7 m/s. The specific energy was 5,2 kW/ m³ of permeate. However, the specific energy is not normative for the production costs of the product water, for this concept, because wind energy is freely available. The investment costs have the largest influence on the production costs and have to be

optimized in the future. By using the method of fitting the required power of the pump and the power curve of the windmill, the best pump can be chosen for a certain wind regime. This can lead to more efficient wind power extraction and even smaller installations.
The quality of product was sufficient for irrigation with salt concentrations lower then 1,200 ppm. The concentration was higher then 500 ppm and therefore not yet sufficient for drinking water purposes. In case the membranes were not compromised the water quality would be improved up to TDS< 175 ppm.
The recovery was low and fixed by the use of the APP/APM combination. The maximum recovery was 20% at a high rotation speed of the pump. This shows that a variable operation of the RO-installation is possible in contradiction to common practice of constant operation. Therefore the combination of APP/APM pumps proved to be useful not only as an energy recovery system but also as a control mechanism for a low recovery at variable wind speed. This low recovery prevents scaling, brings the operating costs down by making use of anti-scalants and acids redundant and increasing the life time of the membranes.

It is advisable to continue testing to investigate the consequences of variable operation for the membranes on long term. Further wind speed registration is needed to be able to predict a certain water production at a given wind regime more precisely. To improve the water quality a proper functioning membranes should be installed. Optimization of the windmill and pump combination should be done using the same method as introduced in this paper. The needed pretreatment and post treatment have to be incorporated into design for subsequent prototype. Also a sustainable solution has to be found for the required inlet pressure for the high pressure pump. Incorporating a wind powered feed pump into the system can be an option. The solution for brine disposal has to be considered in future research as well. The scaling and bio-fouling should be investigated during long term operation.

List of symbols and abbreviations

A	Surface rotor blades [m²]
C	Salt concentration [g/ m³]
c	Scale parameter [m/s]
C_p	Aerodynamic efficiency [-]
E	Energy consumption [kWh/m³]
F	Cumulative distribution function [-]
F	Flushing ratio [-]
f	Probability density function [s/m]
g	Acceleration of gravity [m/s²]
H	Lifting head [m]
IP	Ion product [mol/l]
J	Water flux [m³/ m² s]
K_{sp}	Solubility product [mol/l]
K_w	Membrane water permeability [m]
k	Mass transport coefficient [m/s]
k	Shape parameter [-]
P	Power [W]
p	Feed pressure [Pa]
Q	Flow [m³/s]
T	Torque [Nm]

V	Volume [L]
v	Wind speed [m/s]
$\bar{v}$	Average wind speed [m/s]
Z	Height [m]
α	Stability coefficient [-]
Γ	Gamma function
γ	Recovery [%]
η	Efficiency factor [-]
μ	Absolute viscosity [Pa s]
π	Osmotic pressure [Pa]
ρ	Density [kg/ m³]
Ω	Rotation speed [rad/s]
CP	Concentration Polarization
NDP	Nett Driving Pressure
PV	Photo-Voltaic
RES	Renewable Energy Sources
RO	Reverse Osmosis
SO	Saturation Index
SWRO	Sea Water Reverse Osmosis
TDS	Total Dissolved Solids
TMP	Trans-Membrane Pressure

Acknowledgment

This project would not have been possible without the financial contribution of Mr. and Mrs. Grootscholten, Hatenboer-Water, DEMO and Aqua for All. Also the realization of the first prototype on Curacao was supported by Waterplatform Nederlandse Anitllen & Aruba (WNAA). Special thanks to people at Aqualectra for their assistance during building up and testing of the first prototype. Great gratitude goes out to all the people who contributed to this project in any way.

Literature

1. Fritzmann, C., Löwenberg, J., Wintgens, T., Melin, T., State-of-the-art of reverse osmosis desalination. Desalination, 2007. **216**(1-3): p. 1-76.

2. Al-Sahalia, M., Ettouney, H., Developments in thermal desalination processes: Design, energy, and costing aspects Desalination, 2007. **214**: p. 227–240.

3. Ettouney, H., Design of single-effect mechanical vapor compression. Desalination, 2006(190): p. 1–15.

4. Boyle, G., Renewable Energy; power for a sustainable future. 2004.

5. Kalogirou, S.A., Seawater desalination using renewable energy sources. Progress in Energy and Combustion Science, 2005(31): p. 242–281.

6. Tzen, E., Epp, C., Papapetrou, M. Co-ordination Action for Autonomous Desalination Units Based on RE Systems, ADU-RES. in EWEC 2006. Athens, Greece.

7. Feron, P., Seawater desalintion and wind energy: a system analysis, in Department of physics, laboratory of fluid dynamics and heat transfer, Technische Hogeschool Eindhoven (THE). 1984. p. 134.

8. Garcia-Rodriguez, L., Renewable energy applications in desalination: state of the art. Solar Energy, 2003: p. 381-393.

9. Romero-Ternero, V., García-Rodríguez, L., Gómez-Camacho, C., Thermoeconomic analysis of wind powered seawater reverse osmosis desalination in the Canary Islands. Desalination, 2005(186): p. 291–298.

10. Richards, B.S., Shaefer A. I., Photovoltaic-powered desalination system for remote Australian communities. Renewable Energy, 2003. **28**: p. 2013–2022.

11. Koroneos, C., Dompros, A., Roumbas, G., Renewable energy driven desalination systems modelling. Journal of Cleaner Production 2005(15): p. 449-464.

12. Mathioulakis, E., Belessiotis, V., Delyannis, E., Desalination by using alternative energy: Review and state-of-te-art. Desalination, 2006(203): p. 346-365.

13. Miranda, M.S., Infield, D., A wind-powered seawater reverse-osmosis system without batteries. Desalination, 2002(2002): p. 9-16.

14. Witte, T., Siegfiiedsena, S., El-Allawy, M., WindDeSalter Technology, direct use of wind energy for seawater desalination by vapor compression or reverse osmosis. Desalination, 2003(156): p. 275-279.

15. Liu, C.C.K., Park, J., Migita, R., Qin, G., Experiments of a prototype wind-driven reverse osmosis desalination system with feedback control. Desalination 2002(150): p. 277–287.

16. Thompson, M. Energy Efficiency in Reverse Osmosis Systems. in ADU-RES Seminar. 2005. Hammamet, Tunisia.

17. Betz, A., Introduction to the Theory of Flow Machines. 1966.

18. Lysen, E.H., Introduction to wind energy. 1983: CWD.

19. Vries de, E., TH Rijswijk. 2007. Personal communication.

20. Guda, M.H., The Curaçao Wind Resource Assessment Project paper. 1994, Fundashon Antiyano Pa Energia (FAPE).

21. Bos, F.W.C., Olthof, N., Mechanical testing "Drinking with the wind". 2008, TU Delf.

22. Lisdonk, C.A.C., Rietman, B.M., Heijman, S.G.J., Sterk, G.R., Schippers, J.C., Prediction of supersaturation and monitoring of scaling in reverse osmosis and nanofiltration membrane systems. Desalination, 2001(138): p. 259-270.

23. DuPont, Permasep Products Engineering Manual,. 1992, DuPont Company.

24. Post, J.W., Recovery +, naar een hogere recovery met capillaire nanofiltratie, in Watermanagement. 2000, Delft University of Technology: Delft.

25. Dijk van, J.C., Membrane Filtration. 1991: TU Delft.